Journal of the European Ceramic Society 20 (2000) 1409–1418

Thermal decomposition of asbestos and recycling in traditional ceramics

A.F. Gualtieri[a,*], A. Tartaglia[b]

[a]*Dipartimento di Scienze della Terra, Universitá di Modena e Reggio Emilia, Via S. Eufemia 19, I-41110 Modena, Italy*
[b]*Ferro I.C.C., Casinalbo di Modena, Italy*

Received 10 May 1999; received in revised form 19 October 1999; accepted 31 October 1999

Abstract

Given the known carcinogenic effects, its wide occupational exposures and widespread use in the past, asbestos is considered a general health hazard and a priority treatment for pollution prevention. In this context, asbestos can be entirely transformed to a mixture of non hazardous silicate phases throughout a thermal treatment at 1000–1250°C and to a silicate glass at $T > 1250$°C. These products may be recycled for the production of traditional ceramics. In this paper we describe the recycle of thermally treated asbestos containing materials as a raw material for glass ceramics and traditional ceramics. A significant improvement of the technological properties of porcelainised stoneware, obtained by high sintering of unglazed ceramic bodies, is accomplished by the addition of 5 wt% of an asbestos-based glass ceramic.

Keywords: Asbestos; Fibres; Firing; Raw materials; Silicates; Traditional ceramics; X-ray methods

1. Introduction

Asbestos is a term including amphibole and serpentine minerals which occur in nature as fibres. Amphiboles are double-chain silicates which may assume a fibrous habit being structurally elongated in one preferred crystal direction. Their general formula is $WX_2Y_5Si_8O_{22}(OH)_2$ with X = Na, Y = (Mg, Fe) *riebeckite*; X = Y = (Mg, Fe) *grunerite*; X = Ca, Y = (Mg, Fe) *tremolite*; X = Ca, Y = (Mg, Fe) *actinolite*. Serpentines are 1:1 (a tetrahedral and an octahedral sheet) sheet silicates which may roll to counterbalance the misfit between the tetrahedral and octahedral layer assuming a characteristic fibrous habit with formula $Mg_3(OH)_4Si_2O_5$ (essentially *chrysotile*). Given its favorable properties (incombustibility, low thermal conductivity, alkali and acid resistance, micro-organism resistance, electrical resistance) asbestos has been utilised since ancient times for a large number of applications.

The health hazards associated with exposure to fibrous minerals were unambiguously recognised in the late 1970s although the association between diffuse fibrosis of the lungs and exposure to asbestos was already known in the 1930s.[1] Doll[2] observed increased mortality from lung cancer in UK asbestos workers. The 1972 asbestos standard established a permissible exposure limit (PEL) for asbestos of 2.0 f/ml as an 8 h-time-weighted average (TWA) and the 1986 asbestos standards reduced PEL to 0.2 f/ml. It is now well established that asbestos may induce asbestosis, pleural plaques, pleural effusions, pleural fibrosis, diffuse malignant mesothelioma, and lung cancer. The interaction of asbestos fibres with cells in vivo and in vitro has been the subject of many studies.[3–9] It has been demonstrated that activity among the different fibre types increases with decreasing diameter and increasing fiber length.[10]

Starting from 1980, the US Environmental Protection Agency promoted the removal of asbestos in schools, houses and commercial buildings and later, also European countries followed that policy for the neutralisation of asbestos. Techniques for the neutralisation of asbestos are:

1. ex situ: (i) removal and discharge in toxic waste;(ii) removal followed by thermal inertisation.
2. in situ: (i) full impregnation by viscous media to penetrate and cement the fibers in place;[11] (ii) isolation by chemically inert rigid panels which cover the exposed areas; (iii) chemical inertisation by a foam sprayed on the exposed area that selectively decomposes the asbestos phase.[12]

* Corresponding author. Fax: +39-059-417399.
E-mail address: alex@unimo.it (A.F. Gualtieri).

0955-2219/00/$ - see front matter
PII: S0955-2219(99)00290-3

Although removal and waste disposal is the most widely employed technique, it has many disadvantages: high cost and long times of intervention, large production of toxic waste, high risks of exposure for removal workers, and risk of environmental pollution during and after the operation. Many of the disadvantages can be tackled if the asbestos containing material is thermally treated and recycled. When asbestos is fired at temperatures higher than 1000°C, either serpentine or amphibole species transform into Mg-/Fe-silicates and the products may be recycled at no cost in traditional ceramics with the following advantages: reduction of cost, no production of toxic refuses, decrease of risks of exposure for workers concerned with the disposal operations, and no risk of environmental pollution.

This paper will go through the process of the thermally induced transformation of asbestos containing materials, the production of a glass ceramic, and recycling in porcelainised grès (the top product in the world market of traditional ceramics, which is obtained by high sintering at 1200–1250°C in fast firing cycles of 45–60 min of unglazed ceramic bodies composed of a mixture of white clays kaolinite and illite, sodium and potassium feldspars, and quartz) showing the changes in the microstructure and technological properties of the final product.

2. Experimental procedure

2.1. Materials

Materials selected for the investigation are: (1) a pure serpentine asbestos from the Museum of Mineralogy of the Dipartimento di Scienze della Terra, University of Modena and Reggio Emilia, Italy; (2) a pure amphibole asbestos from the Museum of Mineralogy of Dipartimento di Scienze della Terra, University of Modena and Reggio Emilia, Italy; (3) a commercial asbestos containing material utilised in the past for asbestos-cement pipes (incoherent matrix used for indoor manufacturing); (4) a commercial asbestos-cement for external roofs pipes (coherent matrix used for outdoor manufacturing). The difference between samples (3) and (4) is that in the former, the matrix is incoherent and free asbestos fibres are easily scratched off the surface by hand; in the latter, the matrix is coherent and asbestos fibres can be scratched off the surface only by mechanical tools (i.e. a chisel).

2.2. Characterisation

Characterisation of the samples before and after the thermal treatment was accomplished using X-ray powder diffraction (Philips PW 1710 X-ray diffractometer with a CuK_α radiation in Bragg–Brentano geometry, X-ray fluorescence (Philips PW 1480), thermal analyses TG, DTG, DTA (SEIKO SSC 5200 working in air), and scanning electron microscopy (SEM) (Philips XL 40 with Au sample coating).

3. Results and discussion

3.1. Thermal inertisation

3.1.1. Sample (1)

Sample (1) is pure clinochrysotile (43-662 JCPDS card) with space group $C2/m$ whose powder pattern is reported in Fig. 1a. Its habit, the source of hazard, is clearly fibrous with length of the fibres more than 10 μm and diameter smaller than 1 μm (see the SEM picture in Fig. 2a). The thermal analyses (Fig. 3a) show an endothermic event at $T > 500$°C due to the dehydroxylation of chrysotile and an endothermic event due to the latent heat of crystallisation of forsterite and enstatite according to the reactions:

$$\underset{\text{chrysotile}}{Mg_3(OH)_4Si_2O_5} \overset{500^\circ C}{\Rightarrow} \underset{\text{metachrysotile}}{Mg_3Si_2O7} + 2H_2O \overset{750^\circ C}{\Rightarrow}$$

$$\underset{\text{forsterite}}{Mg_2SiO_4} + \underset{\text{enstatite}}{MgSiO_3}$$

The sample was fired at various temperatures in the range 1000–1350°C and at different heating rates. A complete re-crystallisation to forsterite and enstatite is obtained at 1100°C after 1 h. In fact, the powder pattern of the sample fired at that temperature for 1 h (Fig. 4a) exhibits the peaks of forsterite (340189 JCPDS card, S.G. *Pbnm*) and enstatite (43-662 JCPDS card, S.G. *C2/c*). The SEM picture clearly shows that the morphology of the pre-existing fibres of chrysotile is entirely altered demonstrating that asbestos is definitely transformed into non toxic silicate phases (Fig. 5a).

3.1.2. Sample (2)

Sample (2) is composed of pure tremolite (130437 JCPDS card) with space group $C2/m$ whose powder pattern is reported in Fig. 1b. Again its habit is clearly fibrous with length of the fibres over 10 μm and diameter smaller than 1 μm (Fig. 2b). The thermal analyses (Fig. 3b) mainly show an endothermic event at ca. 950°C due to the dehydroxylation reaction. Again complete re-crystallisation to high temperature phases was obtained by firing at 1100°C for 1 h throughout the following reaction path:

$$\underset{\text{tremolite}}{Ca_2Mg_5(OH)_2Si_8O_{22}} \overset{950^\circ C}{\Rightarrow} \underset{\text{metatremolite}}{Ca_2Mg_5Si_8O_{23}} + 2H_2O \overset{1050^\circ C}{\Rightarrow}$$

$$\underset{\text{diopside}}{2CaMgSi_2O_6} + \underset{\text{enstatite}}{3MgSiO_3} + \underset{\text{cristobalite}}{SiO_2}$$

The powder pattern of the sample fired at that temperature for 1 h (Fig. 4b) exhibits the peaks of diopside (11-654 JCPDS card, S.G. *C2/c*), enstatite (43-662

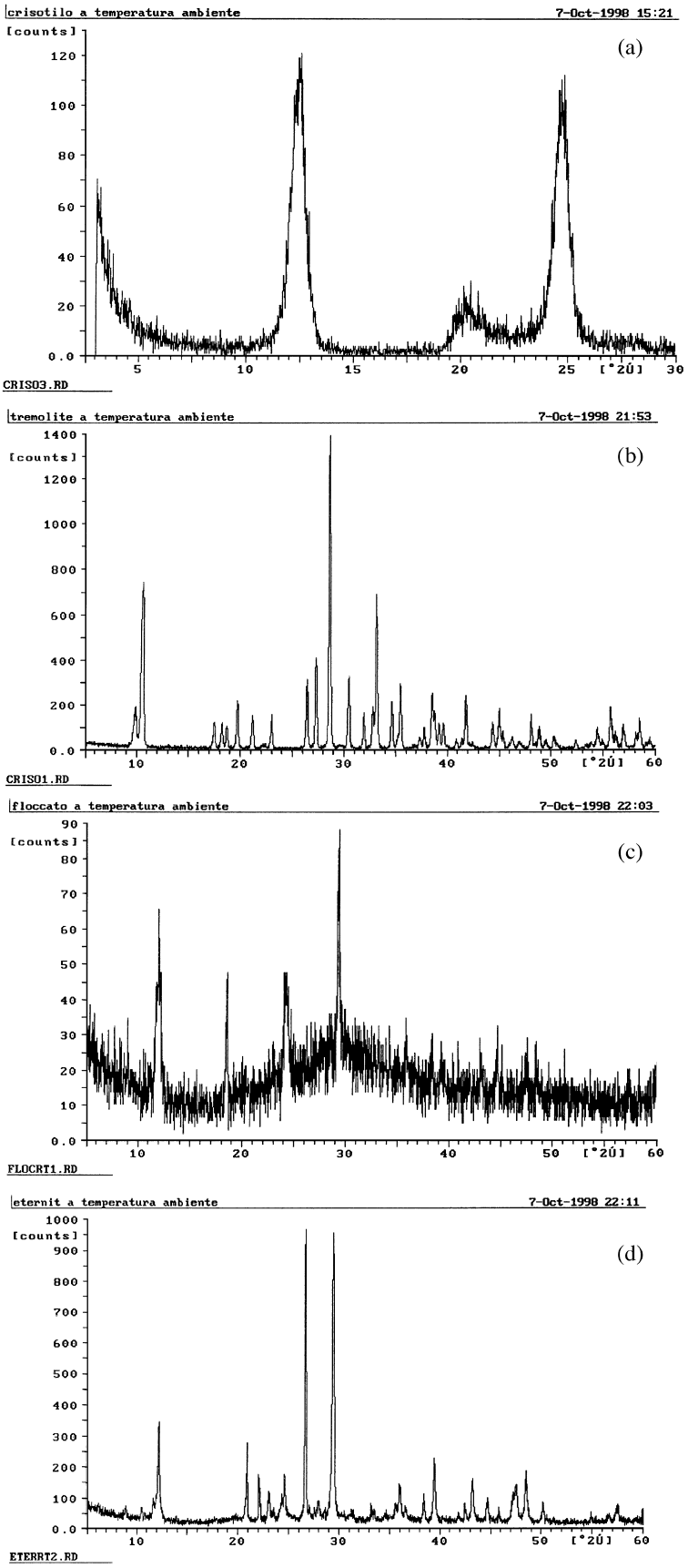

Fig. 1. Room temperature X-ray powder patterns of the investigated samples: (a) sample (1); (b) sample (2); (c) sample (3); (d) sample (4).

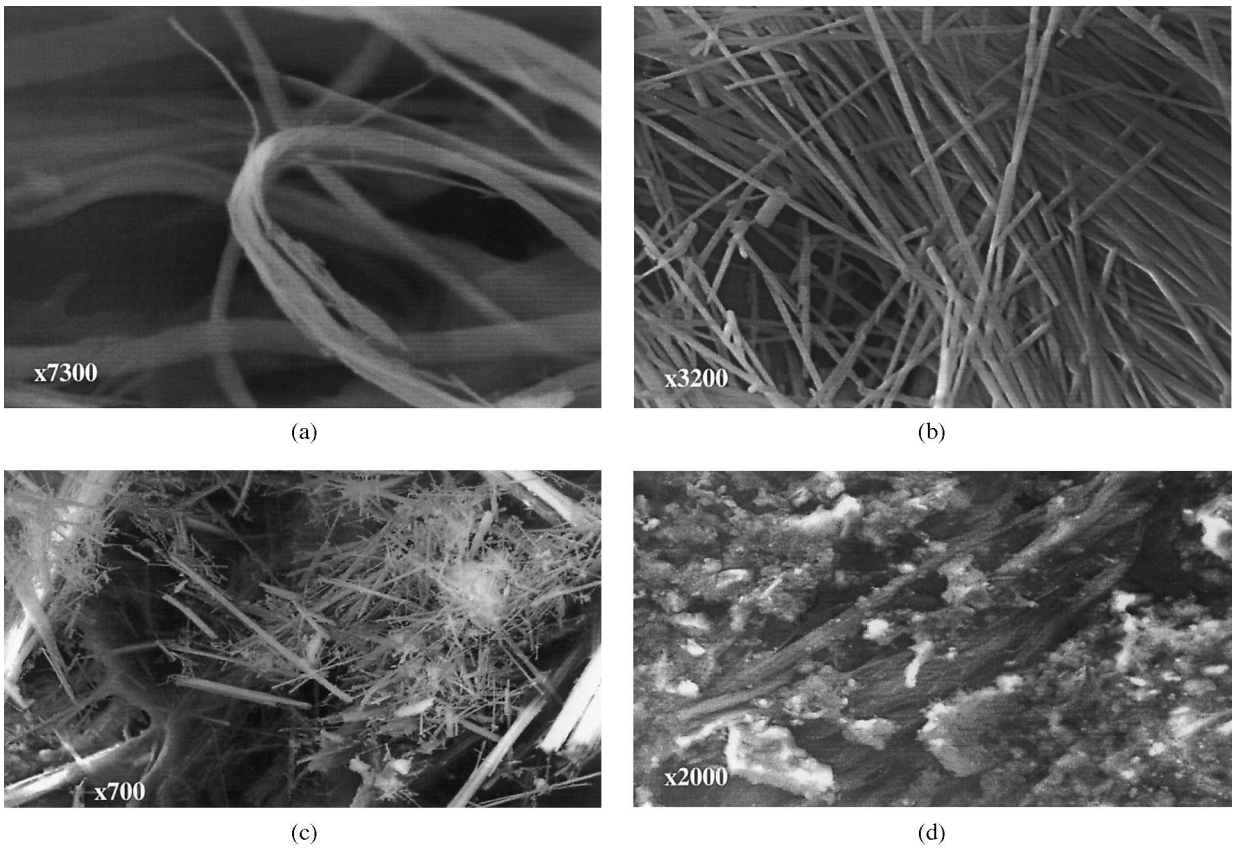

Fig. 2. SEM images of the investigated samples before the thermal treatment: (a) sample (1); (b) sample (2); (c) sample (3); (d) sample (4).

JCPDS card, S.G. *C2/c*), and cristobalite (11-695 JCPDS card, S.G. $P4_12_12$). The SEM picture clearly shows that the fibres of tremolite are again fully transformed into high non toxic silicate phases (Fig. 5b).

3.1.3. Sample (3)

Sample (3) is composed of a mixture of clinochrysotile, calcite (5-586 JCPDS card, S.G. $R\bar{3}c$) and amorphous matter (see the bump centred at about 25–30° 2θ in Fig. 1c). The SEM picture (Fig. 2c) shows that the material is composed of glassy silica fibres, amorphous to diffraction, with interdispersed asbestos fibres and calcite grains. The thermal analyses (Fig. 3c) mainly show an endothermic event at ca. 500–600°C due to the dehydroxylation of chrysotile. A minor, hard to see, endothermic event at higher temperature is due to the decompostion of calcite. Table 1 reports the chemical composition of the calcined sample showing that the glass fibres contain Si, Ca, Mg, Al. Complete transformation occurs at 1100°C after 1 h. The powder pattern of the sample fired at that temperature for 1 h (Fig. 4c) exhibits the peaks of diopside (11-654 JCPDS card, S.G. *C2/c*), gehlenite $Ca_2Al_2SiO_7$ (35-755 JCPDS card, S.G. $P\bar{4}2_1m$), and Fe-forsterite (340189 JCPDS card, S.G. *Pbnm*). A beautiful high magnification SEM picture shows the result of the thermal treatment upon the fibres of tremolite: an intergrowth of silicate crystals (Fig. 5c).

Table 1
Chemical composition of the samples

	SiO_2	CaO	MgO	Al_2O_3	Fe_2O_3	Na_2O	K_2O	TiO_2	MnO	P_2O_5
Sample (3)	41.70	32.48	14.07	8.19	1.66	0.79	0.10	0.37	0.32	0.31
Sample (4)	41.78	35.37	10.54	6.26	4.29	0.82	0.37	0.33	0.15	0.08

3.1.4. Sample (4)

Sample (4) is composed of a mixture of clinochrysotile, calcite (5-586 JCPDS card, S.G. $R\bar{3}c$), quartz (33-1161 JCPDS card, S.G. $P3_22_1$), gypsum (21-816 JCPDS card, S.G. *C2/c*), muscovite (6-263 JCPDS card, S:G: *C2/c*), kaolinite (33-664 JCPDS card, S.G. *C1*), plagioclase (20-548 JCPDS card, S.G. $C\bar{1}$), and cristobalite (39-1425 JCPDS card, S.G. $P4_12_12$) (Fig. 1d). The SEM picture (Fig. 2d) shows asbestos fibres dispersed in the heterogeneous matrix. The thermal analyses (Fig. 3d) show a major endothermic event at $T > 700$°C mainly due to the decomposition of calcite. Table 1 reports the chemical composition of the calcined sample. Complete transformation occurs at 1100°C after 1 h and the corresponding powder pattern (Fig. 4d) shows the peaks of diopside (11-654 JCPDS card, S.G. *C2/c*), gehlenite $Ca_2Al_2SiO_7$ (35-755 JCPDS card, S.G. $P\bar{4}2_1m$), quartz,

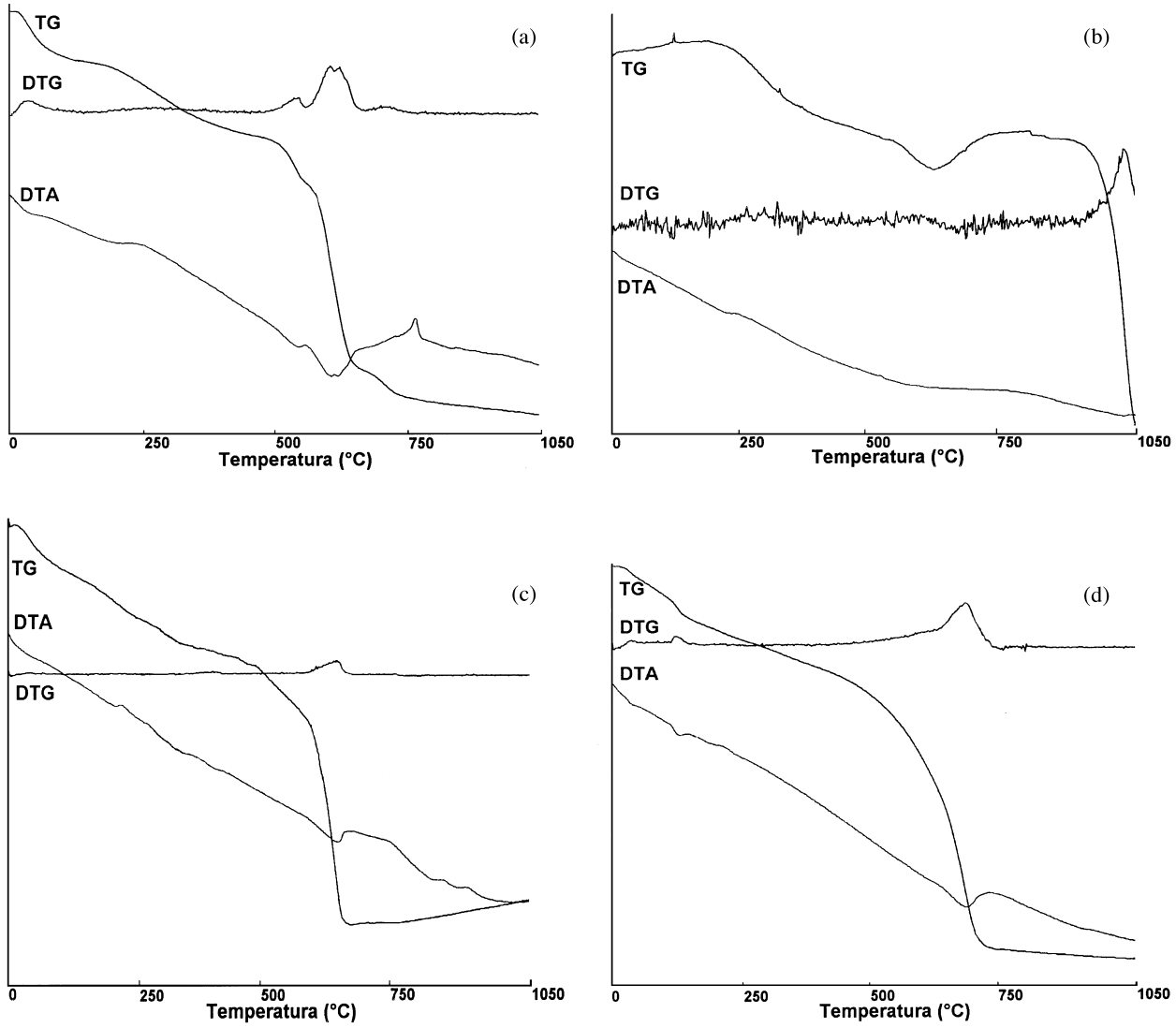

Fig. 3. DTA, TG, and DTG analyses of the investigated: (a) sample (1); (b) sample (2); (c) sample (3); (d) sample (4) collected with $b = 10°C/min$.

and hematite (33-664 JCPDS card, S.G. $R\bar{3}c$). The SEM picture after the thermal treatment shows crystals of the silicate phases in place of the fibres (Fig. 5d).

3.2. Recycle of 1100°C products

The samples (3) and (4) are representative of industrial materials for disposal and thus the recycle in industrial processes will focus only upon the 1100°C fired products of these two samples. At a first stage, the idea was to recycle these inert products directly as a component of the porcelainised grès, the major product in the market of traditional ceramics. To this aim, a standard mixture of porcelainised grés (kaolinite, illite, albite and quartz) was mixed with 5 and 10 wt% of sample (3) or (4), and 0.2 wt% TPF as fluidiser, and milled in alumina jars by addition of 37 wt% water for 15 min. The viscosity of the obtained mud was too high and even addition of 70 and 100 wt% water did not permit the release of the mud from the jar. This behaviour may be explained by the formation of hydrated compounds during the milling process. Both samples (3) and (4) contained CaO as a component of the glass itself and as a product of decomposition of calcite. Not all CaO reacts at temperature to form diopside and gehlenite and some residual CaO in contact with water may yield Ca-hydroxide according to the reaction $CaO + H_2O \Rightarrow Ca(OH)_2$. A gel is formed with a significant increase of the viscosity of the system. The same reaction path is foreseen for MgO whose contact with water yields Mg-hydroxide according to the reaction $MgO + H_2O \Rightarrow Mg(OH)_2$. Addition of extra fluidiser is of no greater help then the use of an excess of water which makes the process clearly non competitive since the costs for successive dehydration would be too high. This solution is thus rejected a priori.

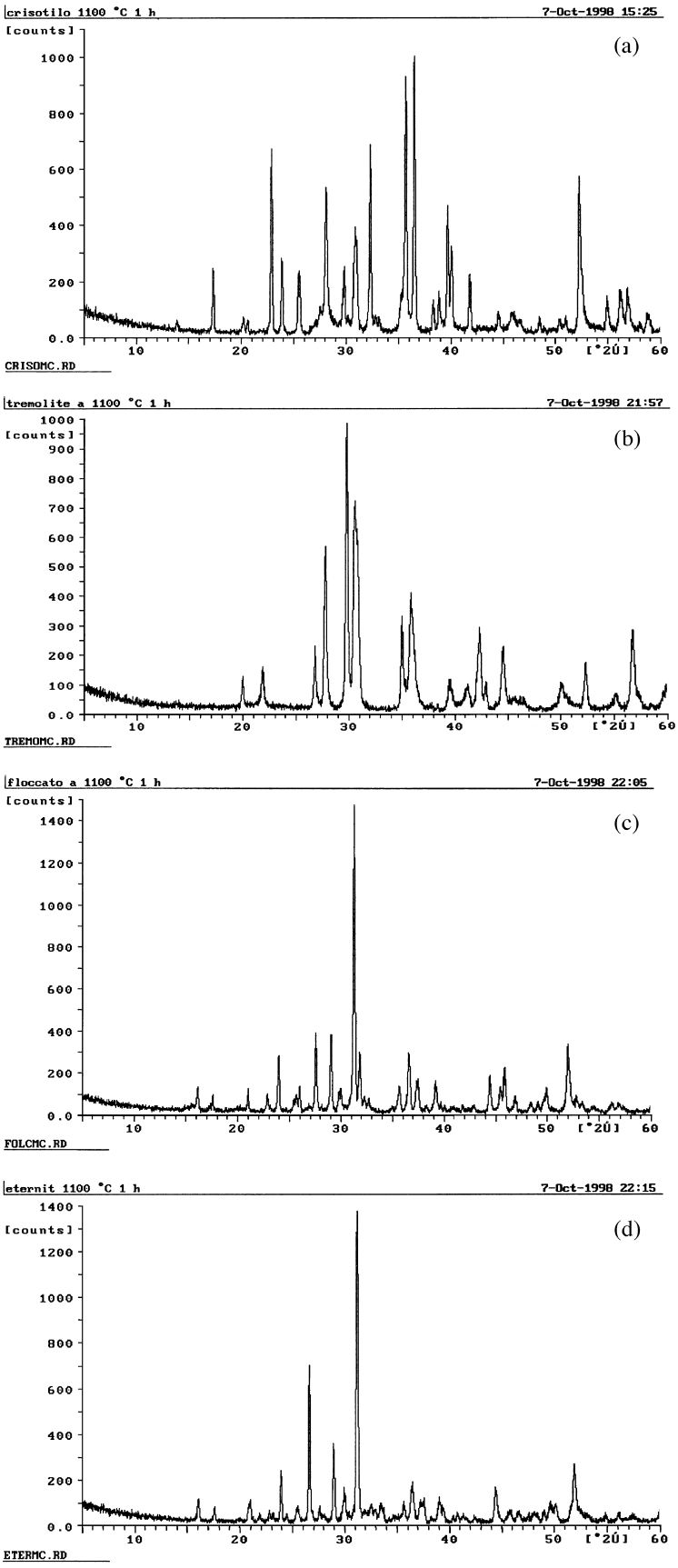

Fig. 4. X-ray powder patterns of the investigated samples after firing at 1100°C for 1 h: (a) sample (1); (b) sample (2); (c) sample (3); (d) sample (4).

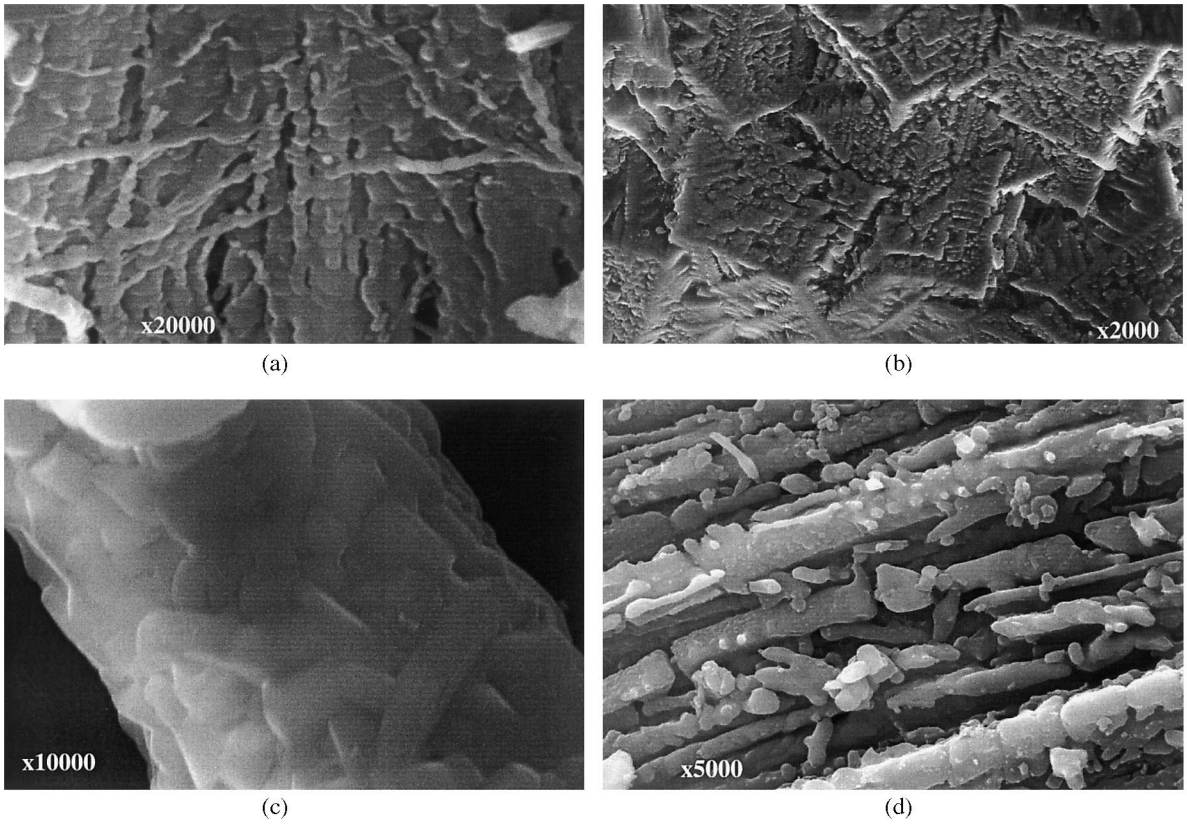

Fig. 5. SEM images of the investigated samples after the thermal treatment at 1100°C for 1 h: (a) sample (1); (b) sample (2); (c) sample (3); (d) sample (4).

3.3. Formation of glass ceramics and recycle in the porcelainised grès

To overcome the problems raised in the previous section, we sought to directly melt the hazardous material to form a glass ceramic. The formulation of a glass ceramic starting from the composition of sample (3) or (4) requires addition of silica and a melting component. To this aim, sample (3) was mixed with 19 wt% of a quartz sand and 3 wt% of Na_2CO_3 and sample (4) was mixed with 30 wt% of a quartz + albite sand. Samples were denominated GC3 and GC4, respectively. Powders were homogenised by dry milling in alumina jars for 15 min, fired in a melt kiln at 1560°C for about 1 h and quenched in water. The product was reground in alumina jars by addition of 50 wt% water and 0.2 wt% TPF for 15 min. The powders were characterised by XRD, DTA, thermodilatometry (TDA): the linear thermal expansion coefficient is well below 90×10^{-7} K^{-1} as required for a raw material for the porcelainised grès. The glass transition takes place at ca. 700°C. The major crystalline phase in the glass ceramic which forms after firing at 1200°C (the temperature of firing of the porcelainised grès) is diopside. Although glass ceramics can be utilised for a number of products, we have focused only on the recycle of sample (3) in the porcelainised grés owing to the importance of this product in the market of traditional ceramics. Because a basic requirement for porcelainised grés is the white colour of the ceramic body (less than ca. 0.5 wt% iron oxides or titanium oxides which colour in firing), the recycle of the glass ceramic obtained from sample (4) which contains 3.3 wt% Fe_2O_3 is limited to low amounts. On the other hand, the recycle of the glass ceramic obtained from sample (3) which contains 1.2 wt% Fe_2O_3 is feasible and promising.

A standard mixture for porcelainised grés was mixed with 5 and 10 wt% GC3. The three mixtures (porcelainised grés with 0, 5 and 10 wt% GC3) were all mixed with 0.2 wt% TPF, respctively, and wet milled (50 wt% water) in alumina jars for 20 min. The mud was dryed at 110°C for 24 h, successively added 6 wt% water and pressed with a load of 400 Kg/cm^2 to form disks of ca. 6×40 mm. Disks were fired in an industrial kiln for 45 min and at a peak temperature of 1215°C. The results of the technological tests on the fired products are reported in Table 2. Fig. 6a–c shows the SEM images of the surface of the three fired products. Rietveld refinements were performed on the fired products using the Rietveld-RIR method[13–16] to achieve a reliable estimate of both the amorphous and crystalline fractions. Fig. 7a–c reports the results of the refinements performed using the program GSAS.[17] The agreement factors between the observed and calculated patterns defined in GSAS[17] are

very good: R_{wp}[17] = 11.7–13.6%; χ^2 = 2.4–3.4; Table 3 shows the results of the quantitative phase analysis with relative standard deviations on each estimate.

The technological and physical properties of the fired products are not significantly altered even by addition of 10 wt% glass ceramic GC3 indicating that the recycle of asbestos containing materials in the process is very promising. Although the differences are slight, addition of GC3 in the mixture should be discussed in the light of the phase composition since a non linear behaviour is observed. The higher values of linear shrinkage and elastic modulus are obtained in the 5 wt% GC3 added product, as well as the lower water absorption. It is clear that the glass ceramic in the mixture behaves as a melting component although a non linear behavior is found. The SEM pictures clearly show that the number and size of pores at the surface of the products is much lower in the CG3 added products indicating that sintering is favoured, especially in the 5 wt% CG3 sample. This is a very important result since the spot resistance[18–20] (standard EN 122, the resistance to marks made by ink), which is highly correlated with the presence of open pores, is significantly improved in the CG3 added products. Concerning the difference in the behavior of the 5 and 10 wt% CG3 samples, Fig. 8 may help. A perfect mass balance of decomposing and forming phases is found if we consider in turn (a) non added sample and 5 wt% CG3 added sample; (b) non added sample and 10 wt% CG3 added sample. Linear variation in the fractions of quartz and diopside (the regression coefficient R^2 is 0.999) reflects a simple variation in the composition due to the addition of CG3. The more CG3 is added, the less quartz and the more diopside are found; the latter crystallizes directly from the glass ceramic. The variation of the fractions of mullite, plagioclase, and glass do not follow a linear trend (R^2 is lower than 0.96). Plagioclase increases with CG3 addition because calcium in CG3 favours the recrystallisation of Ca-plagioclase (anorthite end member as seen also by the Rietveld refinement) at

Table 2
Technological properties of the GC3 added ceramic products

	Undiluted	5 wt% CG3 added	10 wt% CG3 added
Linear shrinkage (%)	7.3	7.7	7.2
Colour (CEC chart)	White A1	White 1	White A1
Water absorption (%)	0.05	0.03	0.05
Apparent density	2.38	2.39	2.36
Elastic modulus E (Gpa)	65.6	70.3	66.7

Table 3
Results of the Rietveld-RIR quantitative phase analysis (esd's in parenthesis)

Phase	Undiluted	GC3 5 wt% added	GC3 10 wt% added
Mullite	4.0(5)	3.7(5)	2.7(4)
Quartz	26.0(8)	23.3(8)	19.7(6)
Plagioclase	10.1(7)	14(1)	16(1)
Diopside	–	0.9(3)	1.8(4)
Glass	59.9(9)	58(1)	59.7(9)
Total	100.0	99.9	99.9

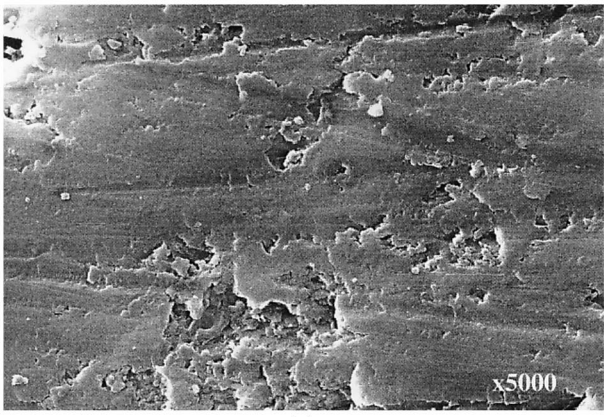

(a)

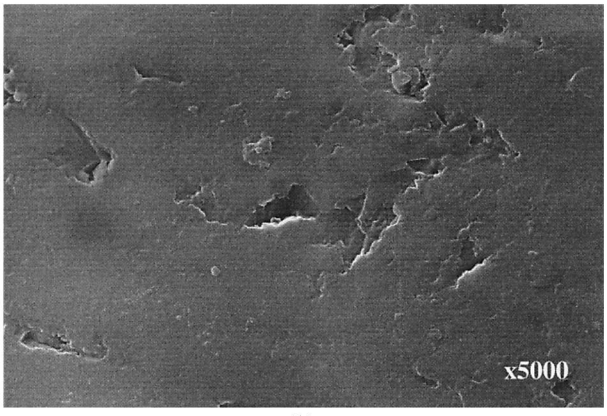

(b)

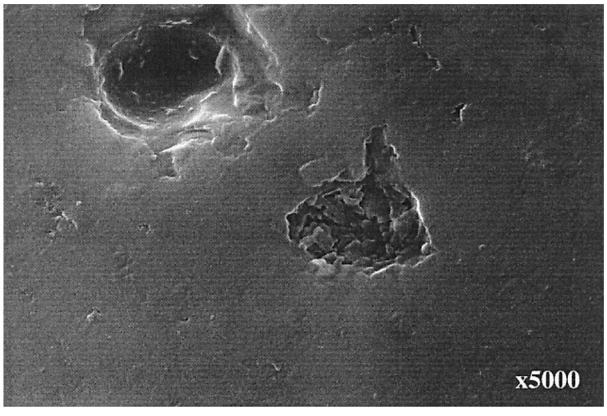

(c)

Fig. 6. SEM images of the surface of the mixtures for porcelainised grès fired at 1215°C: (a) undiluted mixture; (b) 5 wt% GC3 added mixture; (c) 10 wt% GC3 added mixture.

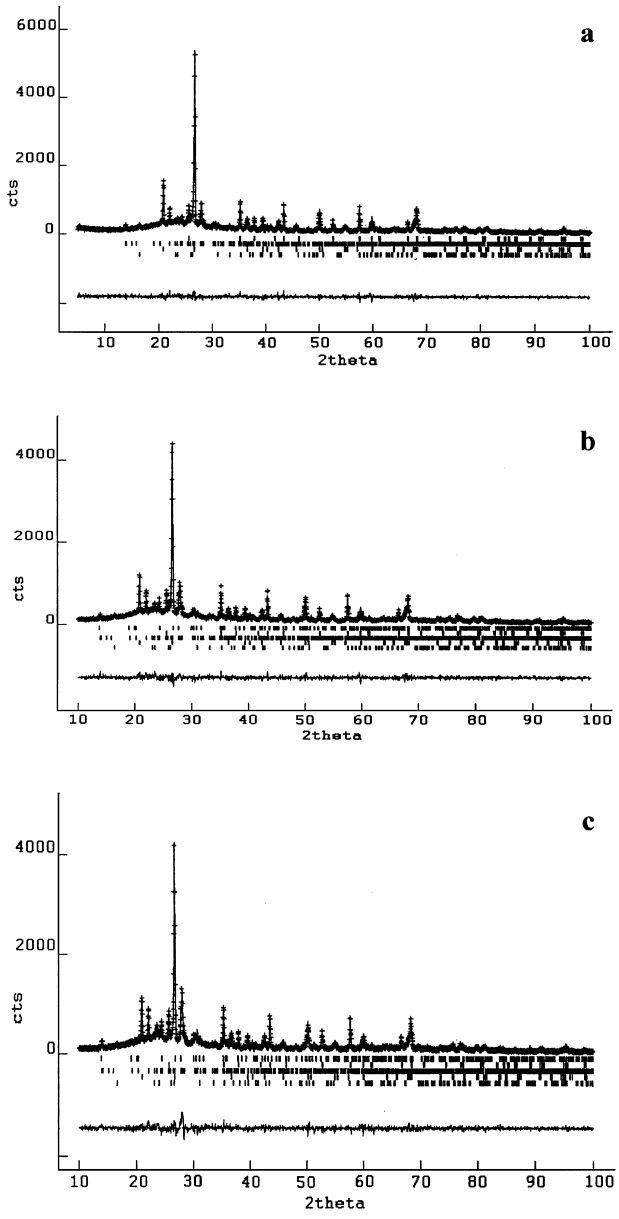

Fig. 7. Observed, calculated, and difference curve of the Rietveld refinements of the mixtures for porcelainised grès fired at 1215°C: (a) undiluted mixture; (b) 5 wt% GC3 added mixture; (c) 10 wt% GC3 added mixture.

the expense of mullite and glass. Such a reaction, taking place at grain boundaries, favours the sintering and changes the microstructure of the system to yield fewer open pores and more reactive grain surfaces. If we consider the original amount of CaO in the glass ceramic CG3 (ca. 22.7 wt%), we have ca. 1.1 wt% CaO available in the system. Part of it is captured in the structure of diopside (0.9 wt% that is 0.2 wt% CaO), and if we consider that the remaining 0.9 wt% CaO forms the anorthite structure, we have ca. 4.5 wt% anorthite corresponding to the extra-amount of Ca-plagioclase. Thus, for these compositions, all CaO from the glass ceramic bahaves as a glass network modifier by entering the diopside and anorthite

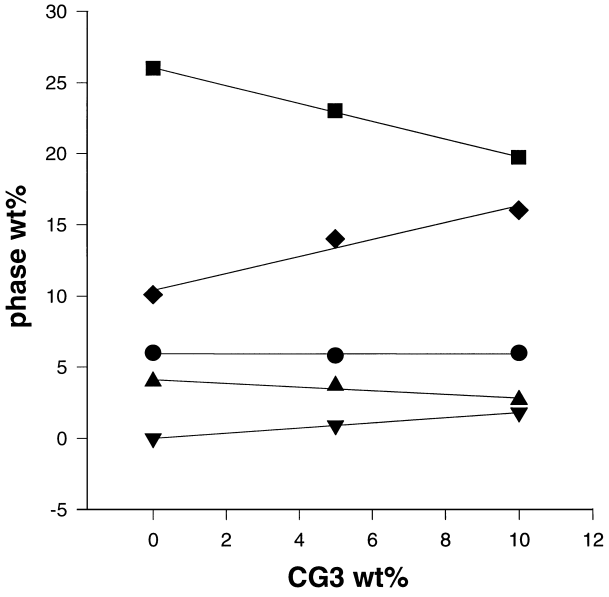

Fig. 8. Rietveld phase compositions of the mixtures for porcelainised grès fired at 1215°C vs amount of added GC3 (wt%). Legend: ■ = quartz; ◆ = plagioclase (albite to anorthite); ● = glass (values are multiplied by 0.1 to keep a proper *y*-axis scale); ▲ = mullite; ▼ = diopside.

structures. Although the same scenario is observed in the sample with 10 wt% CG3 with anorthite forming at the expense of mullite and glass, not all CaO forms anorthite. In fact, by considering the CaO from 10 wt% CG3 (ca. 2.3 wt%) and that 1.8 wt% diopside (0.4 wt% CaO) is formed, ca. 9.4 wt% anorthite should form. Instead only ca. 6 wt% anothite is formed indicating that part of the calcium is in the glass fraction. For that composition, large amounts of anorthite are not in equilibrium in the system which reacts by dissolving it. The result is that the glass fraction increases with respect to the 5 wt% GC3 added sample and consequently all the microstructure and physical properties resemble those of the sample without additions.

4. Conclusion

We succesfully recycled asbestos containing materials as a component of the top product in the market of traditional ceramics: porcelainised grés. Asbestos containing material in an incoherent matrix was added to silica and feldspar and melted to form a Ca, Mg-based glass ceramic (GC3) which in turn was recycled (5–10 wt%) in a mixture for the preparation of porcelainised grès. The asbestos was destroyed and the newlyformed crystalline phases are totally non toxic. The product with 5 wt% GC3 additive shows better technological properites that the sample without additive. The spot resistance is clearly improved since the water absorption is lower and the apparent density is higher. This process is promising because an estimate of the costs for the

recycle is 10 times lower with respect to the costs for disposal as toxic waste. Moreover, another advantage is gained: no hazardous refuses are produced with no risk of environmental pollution.

Acknowledgements

This work is part of the degree thesis of A.T. Financial support was obtained from Italian MURST. We are indebted to the technicians of the Ferro I.C.C. Lab., especially P. Bertocchi for help during the technological tests and the useful discussions.

References

1. Guthrie, G. D., Biological effects of inhaled minerals. *Am. Min.*, 1992, **77**, 225–243.
2. Doll, R., Mortality from lung cancer in asbestos workers. *Brit. J. Indus. Med.*, 1955, **12**, 81–86.
3. Hochella, M. F., Surface Chemistry, structure, and reactivity of hazardous mineral dust, In *Health Effects of Mineral Dusts*. Vol. 28, ed. G.D. Guthrie and B. T. Mossman. Min. Soc. of Am. 1993, pp. 275–305.
4. Langer, A. M., Rubin, I. B. and Selikoff, I. J., Chemical characterization of asbestos body cores by electron microprobe analysis. *J. Histochem. Cytochem.*, 1972, **20**, 723–734.
5. Hume, L. A. and Rimstidt, J. D., The biodurability of chrysotile asbestos. *Am. Min.*, 1992, **77**, 1125–1128.
6. Thomassin, H., Goni, J., Ballif, P. and Touray, J. C., Etude par spectrométrie ESCA des premiers stades de la lixiviation du chrysotile en milieu acide organique. *C.R. Acad. Sci. Paris*, 1976, **283**, 131–134.
7. Jurand, M. C., Ballif, P., Thomassin, J. H., Magne, L. and Touray, J. C., X-ray photoelectron spectroscopy and chemical study of the adsorption of biological molecules on chrysotile asbestos surface. *J. Colloid. Interf. Sci.*, 1983, **95**, 1–9.
8. Guthrie, G.D. and Mossman, B.T. *Health Effects of Mineral Dusts*. Min. Soc. of America, 1993.
9. Stanton, M. F., Layard, M., Tegeris, A., Miller, E., May, M., Morgan, E. and Smith, A., Relation of particle dimension to carcinogenicity in amphibole asbestos and other fibrous minerals. *J. National Cancer Inst.*, 1981, **67**, 965–975.
10. Ross, M., Nolan, P., Langer A.M., Cooper W.C., Helth effects of minerals dusts other than asbestos, In *Health Effects of Mineral Dusts*, Vol. 28, ed. G. D. Guthrie and B. T. Mossman. Min. Soc. of Am. 1993, pp. 361–401.
11. Gualtieri, A. F. A solution for the full impregnation of asbestos: the use of an epoxy polymer resin. *J. Appl. Pol. Science*, in press.
12. Raloff, J., New foam tames an asbestos. *Science News*, 1998, **153**, 5.
13. Artioli, G., Alberti, G., Cagossi, G. and Bellotto, Quantitative determination of crystalline and amorphous components in clinoptilolite-rich rocks by Rietveld analysis of X-ray powder diffraction profiles. In *Atti 1° Convegno Italiano di Scienza e Tecnologia delle zeoliti*, ed. M. Colella. De Frede, Napoli, 1991, pp. 261–270.
14. Gualtieri, A. F. and Artioli, G., Quantitative determination of chrysotile asbestos in bulk materials by combined Rietveld and RIR methods. *Powder Diff.*, 1995, **10**, 269–277.
15. Gualtieri, A. F., Modal analysis of pyroclastic rocks by combined Rietveld and RIR methods. *Powder Diff*, 1996, **11**, 1–10.
16. Gualtieri, A. F. and Zanni, M., Quantitative determination of crystalline and amorphous phase in traditional ceramics by combined Rietveld-RIR method, *Mat. Science Forum*, 1998.
17. Larson, A. C. and Von Dreele, R. B., *GSAS, Generalized Structure Analysis System*. Los Alamos Nat. Lab, New Mexico, LAUR,, 1999 86-748.
18. Brusa, A., Contoli, L. and Dardi, M. In Grés Fine Porcellanato, Grés Porcellanato, Tecnologia, Produzione, Mercato, ed. G. Biff, Faenza Editrice, 1998.
19. Barbieri, L., Bonfatti, L., Ferrari, A. M., Leonelli, C., Manfredini, T. and Settembre Blundo, D., Correlazioni fra proprietà microstrutturali e meccaniche nel gres porcellanato. *Ceramurgia*, 1995, **4**, 187–195.
20. Manfredini, T., Pellacani, G. C., Romagnoli, M. and Pennisi, L., Porcelainised stoneware tile. *Am. Cer. Soc. Bull.*, 1995, **74**, 76–81.